

Geological and Geochemical Prospecting for Gold Mineralisation in Gnimi-Yaboghan, Southwestern Burkina Faso, Western Africa

Ibrahim Ouedraogo¹; Olisa Olusegun.G.²; Saga Sawadogo³

¹Mineral Exploration Programme, Pan African University Life and Earth Sciences Institute (Including Health and Agriculture) University of Ibadan, Nigeria.

²Department of Earth Science, Olabisi Onabanjo University, Ago Iwoye, Nigeria

³Joseph Ki-ZERBO University, Department of Earth's Science, Geoscience Laboratory and Environment, 03 BP 7021, Ouagadougou, Burkina Faso.

Publication Date: 2025/06/03

Abstract: Gold mineralization in Gnimi-Yaboghan, southwestern Burkina Faso, was investigated to enhance understanding of its geological context and exploration potential. Geological mapping at a 1:50,000 scale revealed amphibolite, schist, granitoid, and quartz veins. Mineralogical and geochemical analyses (XRF, ICP-MS) and fire assay techniques identified quartz, feldspar, mica, and accessory minerals. The granitoids were classified as calc-alkaline, peraluminous, and S-type, indicating formation in a subduction zone. A ternary diagram suggested a hydrothermal submarine origin for the quartz veins. Lithophile elements (K, Rb, Ba, Sr) showed a genetic link between quartz veins and metasedimentary rocks, with metamorphic fluids likely responsible for gold deposition. Gold content was very low in granitoids (<0.002 ppm) but reached up to 9.9 ppm in quartz veins, confirming them as the primary gold-bearing structures. This study supports previous findings that most gold in Burkina Faso is hosted in quartz veins and highlights the significance of hydrothermal processes in mineralization.

Keywords: Geochemical Prospecting, Gold Mineralisation, Hydrothermal Fluid, Structures, Burkina-Faso.

How to Cite: Ibrahim Ouedraogo; Olisa Olusegun.G.; Saga Sawadogo (2025). Geological and Geochemical Prospecting for Gold Mineralisation in Gnimi-Yaboghan, Southwestern Burkina Faso, Western Africa. *International Journal of Innovative Science and Research Technology*, 10(5), 3084-3097. <https://doi.org/10.38124/ijisrt/25may1828>

I. INTRODUCTION

Gold is a precious metal with an increasing demand worldwide. It can occur in different geological environments associated with different types of rocks formed at different geological conditions. The study of gold fields and geological work documented by the Burkina-Faso Geological Survey indicates that orogenic gold deposit is the main source for gold production (Goldfarb et al.,2001) . Beziat et al.,2008) revealed that Gold deposits in Burkina-Faso are of the orogenic gold type hosted by quartz veins. They occur mostly in lithological contacts and quartz veins related to brittle-ductile shear zones (Baratoux et al.,2015 ; Markwitz et al.,2016) . Determination of appropriate structural patterns and hydrothermal processes is very important in gold exploration .(Ilboudo et al.,2018) reported that the gold mineralization at Belahourou, northern Burkina-Faso, is related to hydrothermal fluids which are associated with the plutonic rock's emplacement. With the aid of field data, mineralogical, geochemical and ore fluid data (Oke et al.,2014)carried out a study in the mineralogical and

geochemical characterization of some quartz veins in Northwestern Nigeria. They suggest that the ore fluids responsible for the mineralization may come from fractures, metamorphic and sedimentary rocks. Studies have been carried out to examine the relationship between structures and gold mineralization Gustafson (1989).

Based on the genesis, two main types of gold can be described (Nguimatsia et al.,2017): syngenetic gold, which is formed at the same time as host rocks and epigenetic gold, which postdates the host rocks' formation Lovering (1963).

The study area is located in the Boromo greenstone belt and covers longitudes 2°55'45''W to 2°56'55''W and latitudes 11°17'30''N to 11°19'30''N (Figure 1). Geologically, the southwest part is occupied by Paleoproterozoic Formations (Ouiya et al.,2016) and is characterized by volcanic and sedimentary rocks (Koffi et al.,2017; Ali et al.,2022).

The Paleoproterozoic domain of the western Burkina Faso revealed three greenstone belts with N-S orientation: the Houde, Banfora and the Boromo greenstone belts (Castaing et al.,2003). Most gold deposits in Burkina-Faso are located in the Paleoproterozoic domain. They are of orogenic gold type controlled by structures in shear zones with a NW-SE orientation and hosted by quartz veins (Ouedraogo et al.,2023).

Gold occurrences have been reported in south-west Burkina Faso with the preponderance of artisanal miners working on different geological units within the area. However, these artisanal miners lack the geological knowledge to understand the lithological characteristics of the geological units hosting the Au mineralization potential of lithologies in the study area.

This study aims to determine lithologies, mineralogical, geochemical characteristics and mineralisation potential.

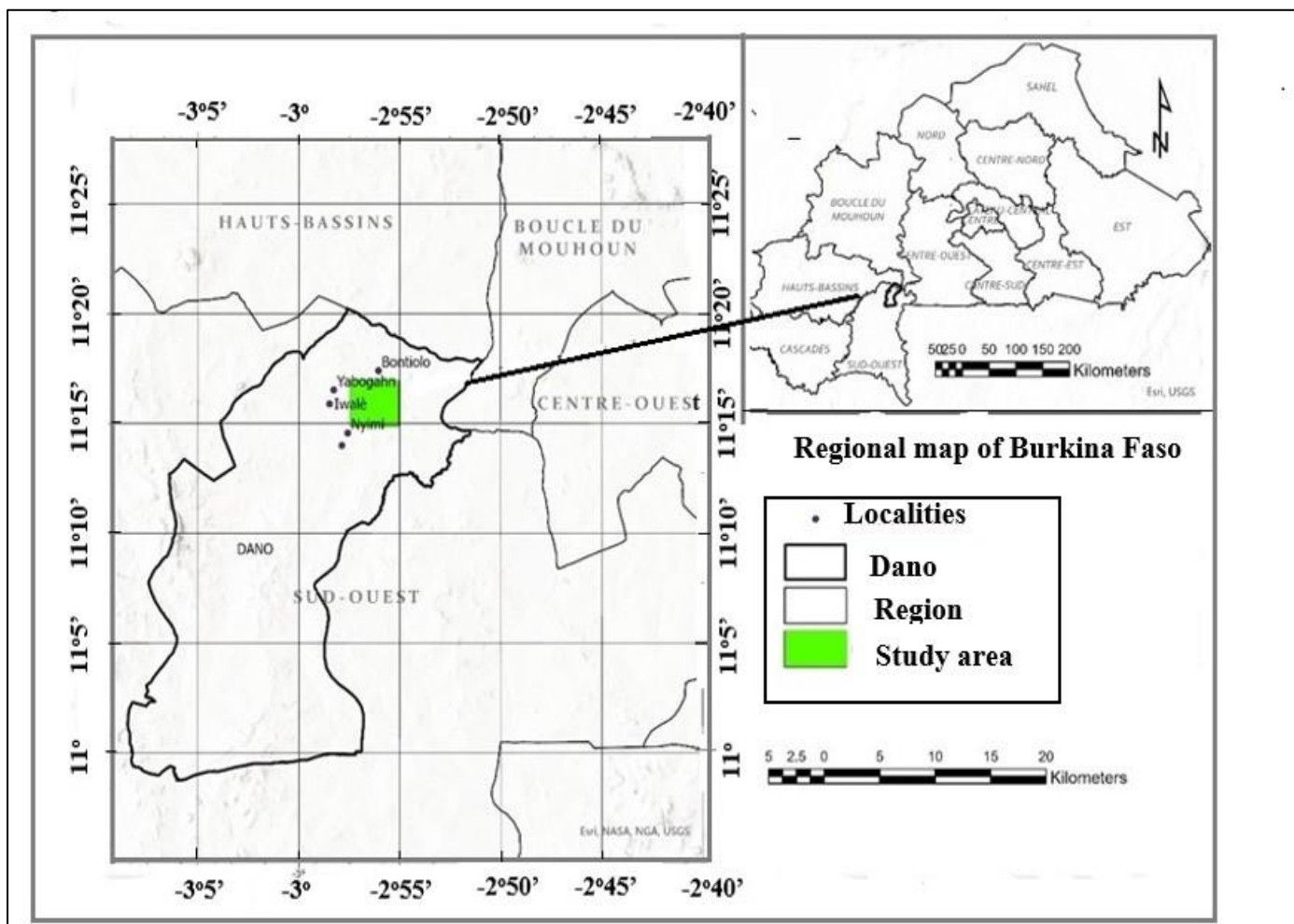


Fig 1 Location Map of the Study Area

II. GEOLOGICAL SETTING

The West African Craton (WAC), located at the northwestern margin of Gondwanaland, comprises two major Early Proterozoic regions: the Archean and the Reguibat Shield (Ledru et al.,1992). The Archean consists largely of greenstone belts with intense volcanic activity between 2.25–2.19 Ga (Block et al.,2015), contrasting with the Precambrian TTG (Tonalite-Trondhjemite-Granodiorite) plutonic rocks Nancy (1990). The Precambrian crust of West Africa formed through three major orogenic events: Liberian (3.0–2.5 Ga), Eburnean (2.5–1.8 Ga), and Pan-African (~0.6 Ga).

Archean and Proterozoic formations are found in the northern Reguibat Rise and southern Leo Rise (Boher et al.,1992). The Archean Man Domain and the

Palaeproterozoic Birimian are dominant in the southern WAC (Ganne et al.,2014). Ivory Coast comprises Archean and Paleoproterozoic formations (Gaby et al.,2000), while southern Mali consists of folded, weakly metamorphosed volcano-sedimentary rocks with Eburnean features (Toukara et al.,2017).

The WAC is primarily composed of Paleoproterozoic formations of the Man Shield (Gaby et al.,2000), with volcanic belts and sedimentary basins of the Birimian Group, subdivided into Lower and Upper Birimian (Abouhami et al.,1990; Oberth et al.,1998; Dabo and Aifa (2011)). The Birimian greenstone belt is renowned for its gold richness (Chris (2013) and has undergone three deformation events: NW–SE compression (D1), sinistral strike-slip (D2), and dextral reactivation (D3) (Augustin et al.,2015).

Volcanic activity dominated early Paleoproterozoic times (2250–2100 Ma) (Blok et al.,2016) , with shear zones in sedimentary terrains Jessell (2018) and granitoid intrusions of varying ages (Naba et al.,2004; Reisberg et al.,2015) . In NE WAC three granitoid types are identified: TTG, non-foliated granite, and alkaline granite Jessell (2018).

Over 80% of Burkina Faso lies in the Baoulé-Mossi domain (Gaby et al.,2000) , dominated by Birimian rocks. Granitoid intrusions in metavolcanic/metasedimentary rocks around 2.1 Ga accompanied Birimian deformation (Hien et al.,2004) . Tarkwaian sediments, mafic tholeiites, and calc-alkaline magmas appear in Ivory Coast, Ghana, and Burkina

Faso (Metelka et al.,2011 ; Chudasama et al.,2015; Ludtke et al.,1999) .

The Boromo belt shows greenschist metamorphism and gold mineralisation in Larafella and Poura (Beziat et al.,2000) . Three types of metamorphism have been identified in the Paleoproterozoic domain: high-temperature metamorphism, the volcanic and volcano-sedimentary metamorphism, and amphibolite metamorphism, which is responsible for orogenic gold deposits(Gaby et al.,2000). Four deformation phases (D1–D4) exist, with D1 (E–W trend) linked to most gold deposits like Mana, Wona-Kano, and Julie (Ilboudo et al.,1781; Masurel et al.,2021) .

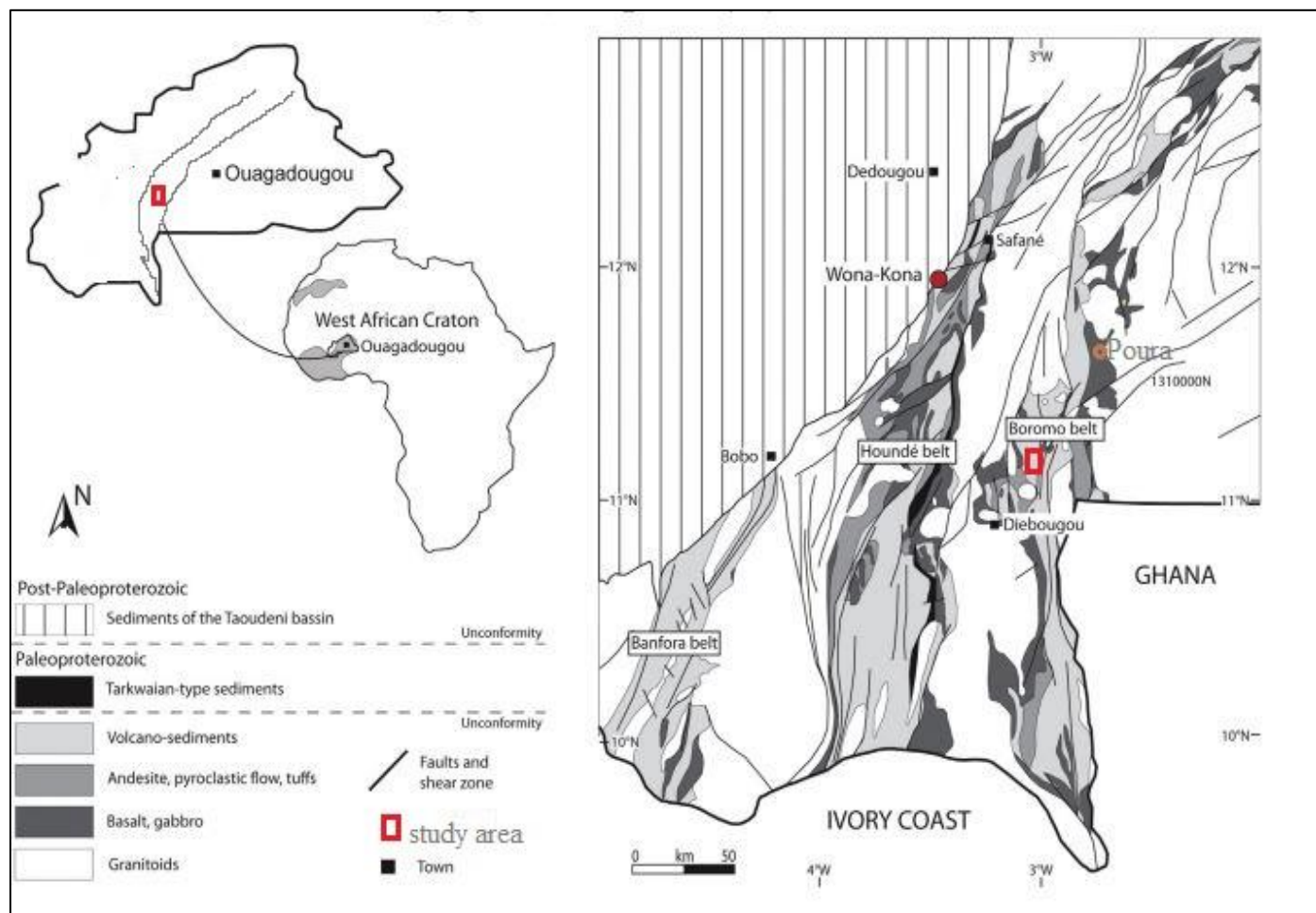


Fig 2 Regional Geology of Western Burkina Faso Showing Major Shear Systems and the Study Area. Modified from after (Baratoux et al.,2011).

III. MATERIALS AND METHODS

Detailed geological mapping at a 1:50,000 scale was conducted, and 34 rock samples were collected from outcrops, using joints and exfoliation surfaces to access fresh materials. Twelve thin sections were prepared and analyzed petrographically at the University of Ibadan, with photomicrographs taken of key features. Three representative samples underwent mineralogical analysis using a JEOL JSM 6610 SEM-EDS at the University of the Free State, South Africa. Major oxides in seven granitoid samples were analyzed via XRF, while trace elements from seven granitoids and five quartz vein samples were analyzed by

ICP-MS at ALS Geochemistry, Canada. Gold concentrations were determined by fire assay, and all geochemical data were processed using Petrograph software.

IV. RESULTS

➤ Geology and Petrography

Four lithological units were observed in the study area: schist, amphibolite, granite and quartz veins. The schist occurs as mafic fine-grained and altered rocks (Figure 3a and 3b). Petrographically, it is composed of plagioclase, amphibole, K-feldspar and biotite (Figure 4a and 4b). Backscatter Electron Images (BSE) revealed the presence of

pyrite, mica, apatite, calcite, titanite, pyroxene and arsenopyrite (Figure 5a and 5b). The amphibolites are green in color and a fine grain texture was observed (Figure 3c). They occur in the southeastern part with amphibole as the main mineral present with accessory quartz (Figure 4c.). BSE images revealed the presence of ilmenite, rutile, titanite, pyroxene, calcite, apatite, garnet and arsenopyrite (Figure 5c and 5d).

Granitic rocks are the most abundant rock type in the study area. They are grey with granular texture (Figure 3d and 3e). Petrographic analysis reveals the presence of plagioclase, quartz and biotite with rare amphibole (Figure 4e and 4d). BSE images revealed the presence of apatite, pyroxene, garnet, titanite, ilmenite, rutile and zircon (Figure 5e and 5f). The quartz veins are the youngest lithological unit in the area. The quartz vein type appears as massive veins with milky white color (Figure 3f.). Petrographic analysis reveals the presence of quartz (Figure 4f.).

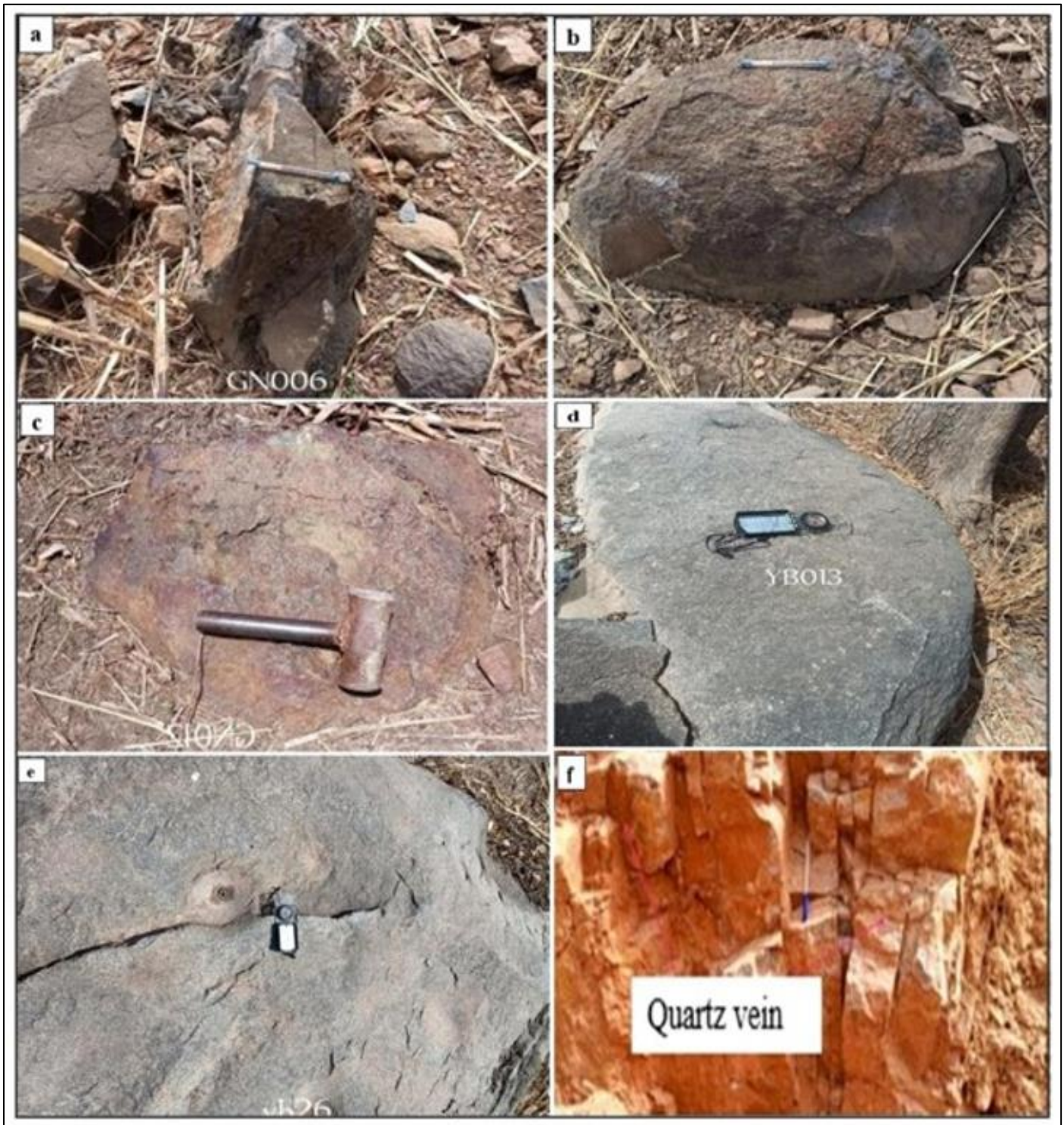


Fig 3 (a,b) Field photograph of schist; (c) Field photograph of altered amphibolite;(d,e) Field photograph of granitoids without alteration;(f) Field photograph of quartz vein.



Fig 4 (a,b) Photomicrograph of schist showing quartz (Qtz), K-feldspar (K-fs), amphibole (Amp) and Biotite (Bt); c photomicrograph of amphibolite showing Quartz (Qtz) and amphibole (Amp) ; (d,e) Photomicrograph of granitoids showing quartz (Qtz), biotite (Bt), plagioclase (Pl), K-feldspar (K-fs); and amphibole (Amp) ; (f) Photomicrograph of quartz vein showing quartz (Qtz).

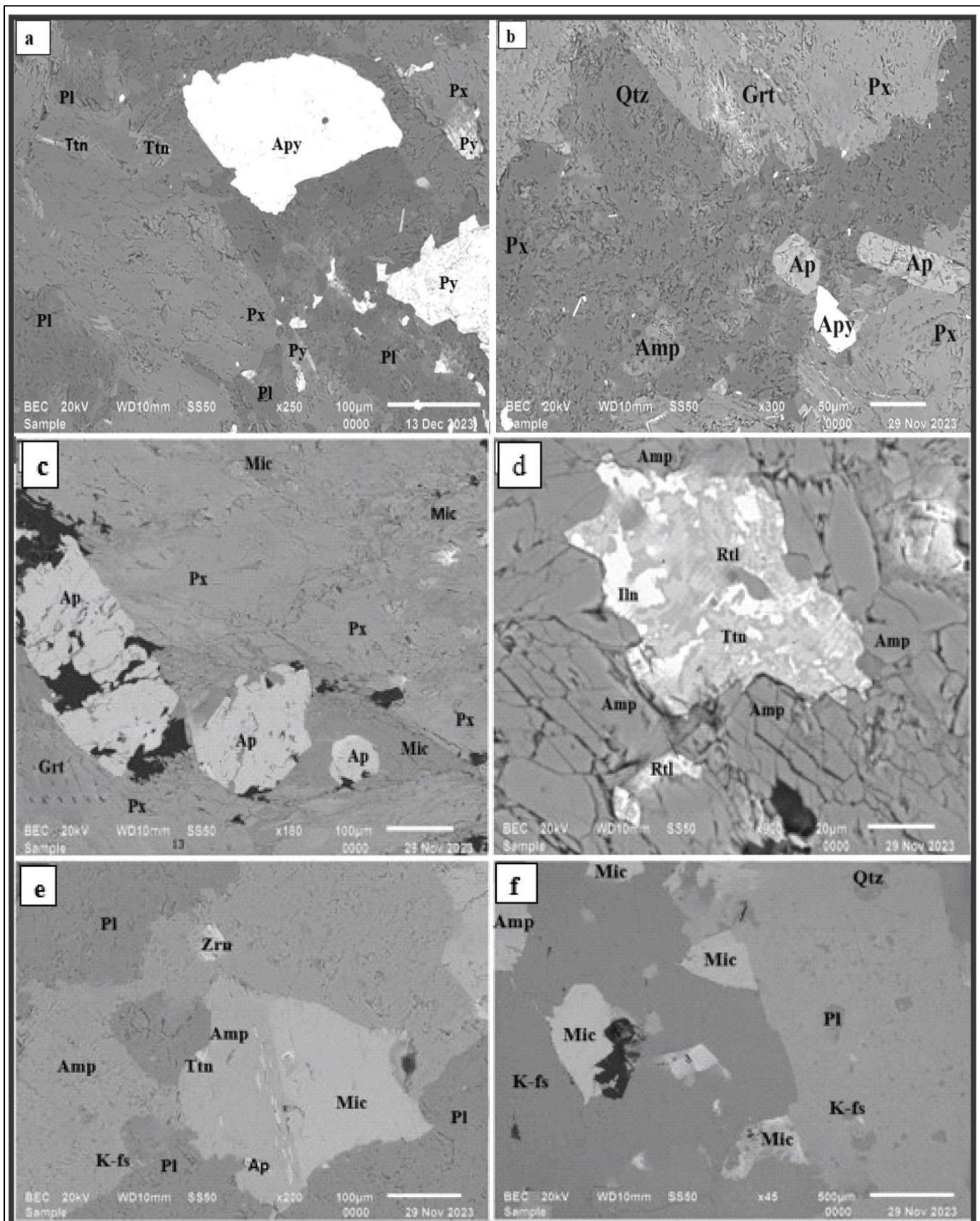


Fig 5 (a,b) BSE image of schist showing the presence of, pyroxene (Px), titanite (Ttn), plagioclase (Pl), arsenopyrite (Apy), pyrite (Py), amphibole (Amp), mica (Mic), garnet (Grt), apatite (Ap), quartz (Qtz), K-feldspar (K-fs), and calcite (Cal); (c,d) BSE image of amphibolite showing the presence of pyroxene (Px), apatite (Ap), garnet (Grt), mica (Mic), amphibole (Amp), rutile (Rtl), ilmenite (Ilm), and titanite (Ttn). (e,f) BSE image of granitoids showing the presence of amphibole (Amp), zircon (Zrn), mica (Mic), K-feldspar (K-fs), plagioclase (Pl), quartz (Qtz).

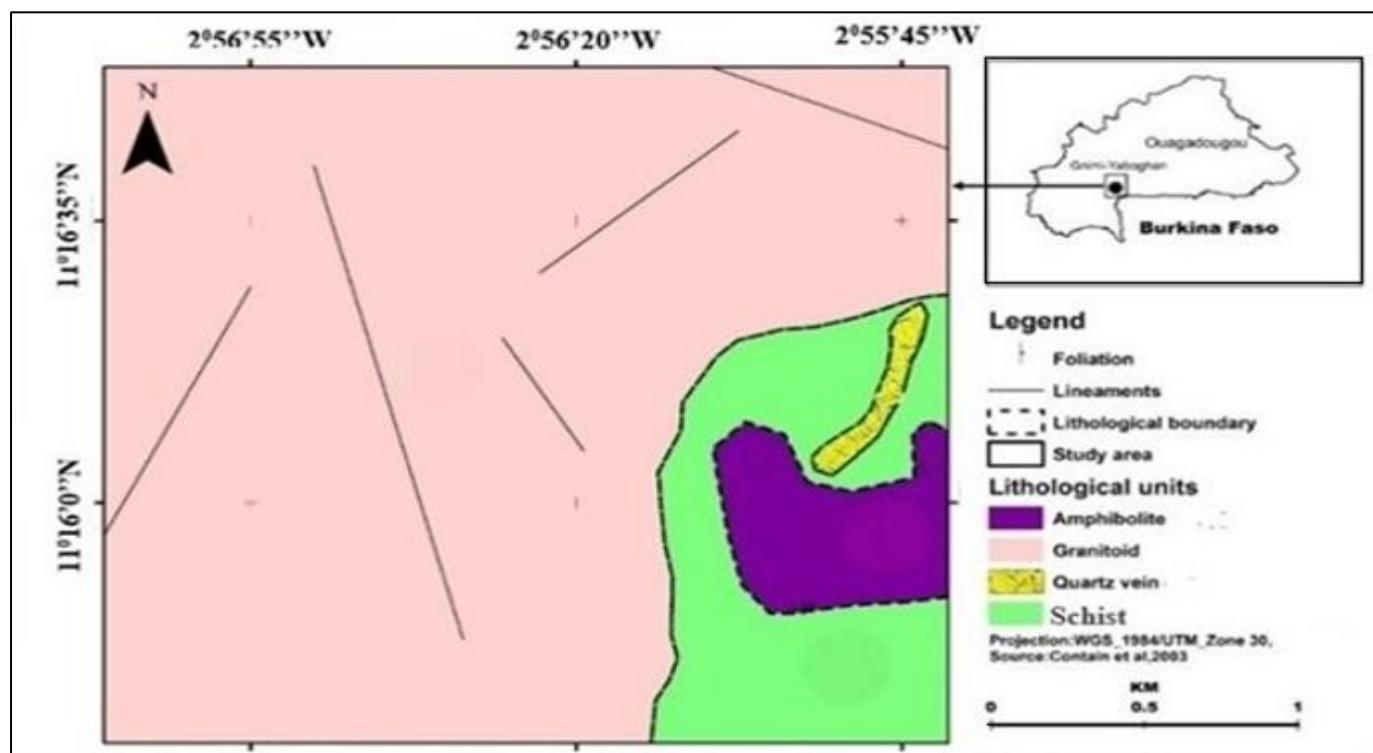


Fig 6 Geological Map of the Study Area Showing the Different Lithology.

➤ *Geochemistry*

• *Granitoids*

The geochemical analysis of the granitic rocks from the study area shows a wide range of major and trace elements. The rocks are siliceous, with SiO₂ contents between 66.99% and 71.49%. Other major oxides include Al₂O₃ (14.23–15.32%), CaO (2.48–4.11%), Na₂O (2.83–3.37%), K₂O (3.26–4.02%), Fe₂O₃ (2.99–5.22%), MgO (1.45–3.12%),

MnO (0.05–0.08%), TiO₂ (0.26–0.48%), and P₂O₅ (0.10–0.19%).

Trace element concentrations vary significantly: Ag (0.05–0.12 ppm), Ba (600–980 ppm), Ce (45.2–49.3 ppm), Co (7.9–15.6 ppm), Cr (54–90 ppm), Cs (4.03–8.51 ppm), Cu (8.2–16.5 ppm), Ga (15.7–17.75 ppm), Li (44.5–72.3 ppm), Nb (5.4–6.6 ppm), Ni (13.7–24.3 ppm), Pb (18.7–33.3 ppm), Rb (100.5–149.5 ppm), Ta (0.5–0.83 ppm), Th (6.41–17.05 ppm), U (1.2–17.4 ppm), and Y (10.1–24.8 ppm). Gold values were below the detection limit of 1 ppb.

Table 1 Elemental Composition in Granitoids around Gnimbi-Yabaghan, Burkina-Faso

Sample	YB13	YB15	YB012	YB26	YB20	YB21	YB23
SiO ₂ (%)	69.91	69.92	70.21	66.99	68.84	67.93	71.49
TiO ₂ (%)	0.28	0.3	0.32	0.48	0.34	0.31	0.26
Al ₂ O ₃ (%)	14.74	14.26	14.46	15.32	14.44	14.24	14.23
Fe ₂ O ₃ (%)	3.4	3.36	3.62	5.22	3.79	3.48	2.99
MgO (%)	1.45	1.56	1.69	3.12	1.85	1.69	1.48
MnO (%)	0.05	0.05	0.06	0.08	0.06	0.06	0.05
CaO (%)	2.98	2.8	2.9	4.11	2.83	2.78	2.48
Na ₂ O (%)	3.03	3.25	3.12	2.83	3.06	3.09	3.37
K ₂ O (%)	3.26	3.57	3.87	3.43	4.02	3.7	3.76
P ₂ O ₅ (%)	0.11	0.11	0.12	0.19	0.13	0.12	0.1
LOI (%)	0.46	0.66	0.58	0.68	0.48	0.93	0.56
Ag (ppb)	0.06	0.06	0.12	0.07	0.07	0.05	0.08
As(ppm)	1.9	1.1	2.1	0.8	1.4	1.9	1.7
Ba(ppm)	830	980	900	790	810	600	930
Be(ppm)	1.7	1.44	1.69	1.33	1.79	1.83	1.81
Bi(ppm)	0.11	0.06	0.16	0.03	0.2	0.19	0.21
Cd(ppm)	0.33	0.22	0.3	0.2	0.15	0.11	0.28
Ce(ppm)	46.4	47.4	47.3	47.7	49.3	49.3	45.2
Co(ppm)	9.9	7.9	10.2	15.6	11.3	9	9.7
Cr(ppm)	65	54	59	90	71	58	55

Cs(ppm)	4.53	5.74	7.28	4.03	8.51	8.31	7.78
Cu(ppm)	8.4	10.3	11.5	16.5	12.1	8.2	10
Hf(ppm)	3.4	3.5	3.2	3	3.5	3.9	3
Hg(ppm)	<0.005	0.014	0.006	0.005	<0.005	0.006	0.01
Li(ppm)	58.8	49.7	59.5	44.5	66.6	56	72.3
Na(ppm)	2.69	2.66	2.67	2.52	2.7	2.54	2.72
Nb(ppm)	6.3	5.4	6.1	6.6	6.5	6	6
Pb(ppm)	19.9	20.3	33.3	18.7	19.3	21.5	19.5
Rb(ppm)	120	125.5	128.5	100.5	133	149.5	120.5
Y(ppm)	21.7	10.1	20.8	14.3	20.7	12.9	24.8
Au(ppm)	<0.001	<0.001	<0.001	<0.001	<0.001	<0.001	<0.001

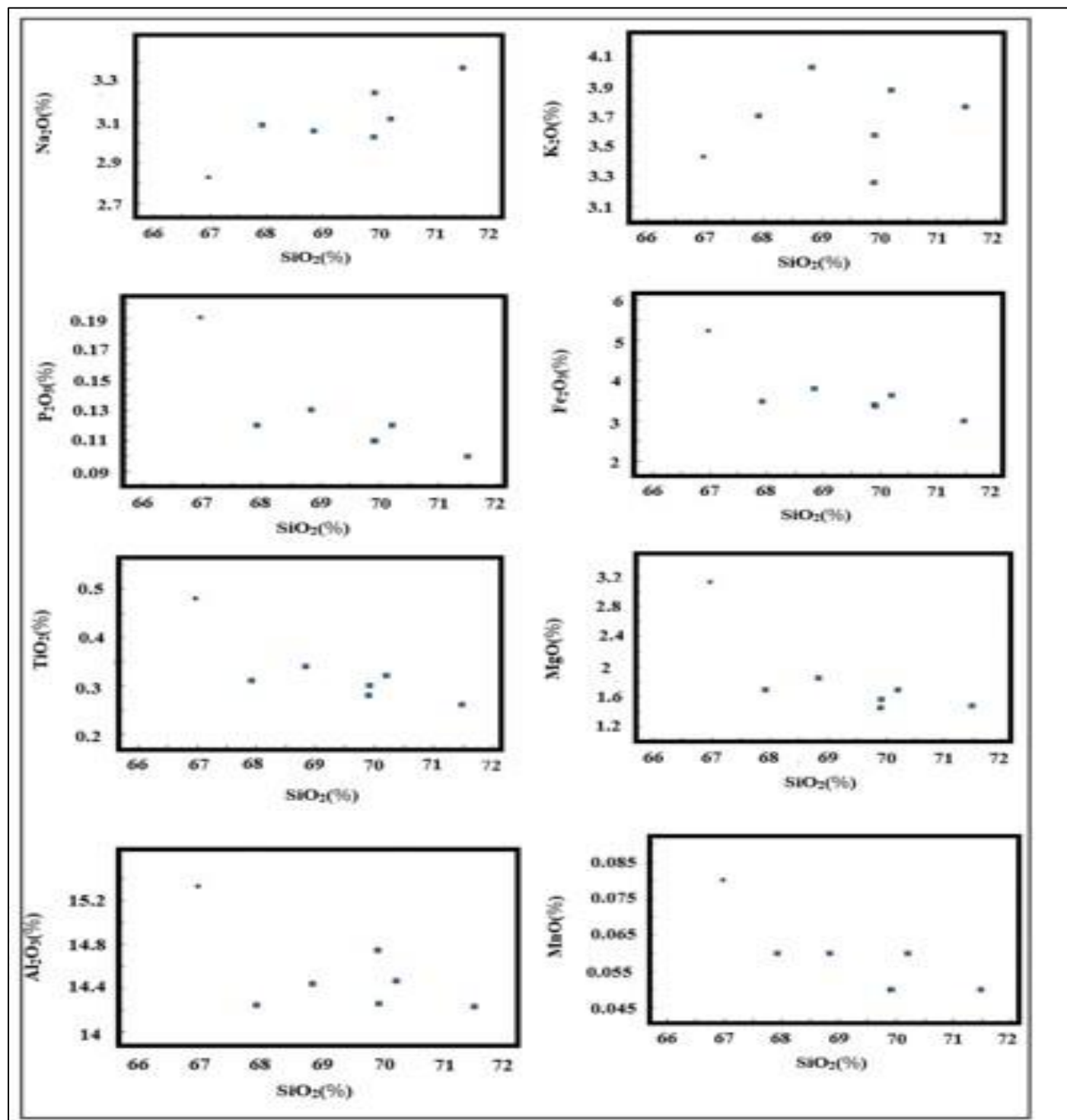


Fig 7 Harker Diagram for Granitic Rocks

Harker plots (Figure 7) show negative correlations of P_2O_5 , Al_2O_3 , MnO , MgO , TiO_2 , and CaO with SiO_2 , and positive correlations of Na_2O and K_2O with SiO_2 . This indicates that the granitoids belong to the same magmatic suite and have undergone fractional crystallization, with early removal of ferromagnesian phases. On the TAS diagram (Figure 8a) (Cox et al.,1979), most granitoids plot in the granite field, with one in the granodiorite field. The AFM diagram (Figure 8b) confirms a calc-alkaline affinity (Irvine et al.,1971). The SiO_2 vs K_2O diagram of Peccerillo and Taylor (1976) places all samples in the High-K calc-alkaline

series (Figure 8c). The $Al_2O_3/(Na_2O+K_2O)$ vs $Al_2O_3/(CaO+Na_2O+K_2O)$ diagram (Frost et al.,2001) shows a peraluminous character (AI, ASI up to 1), with ASI values between 1.4–1.8, indicating S-type granites Frost (2008) (Figure 8d). These granites likely result from crustal anatexis, not mantle-derived sources Debon and Fort (1983). According to classification of McDonald and Katsura(1964), all samples are subalkaline (Figure 9a). Tectonic setting plots (Pearce et al.,1984) (Figure 9b and 9c) place them in volcanic arc and syn-collisional granite fields, suggesting formation in subduction-related environments Pearce (1996).

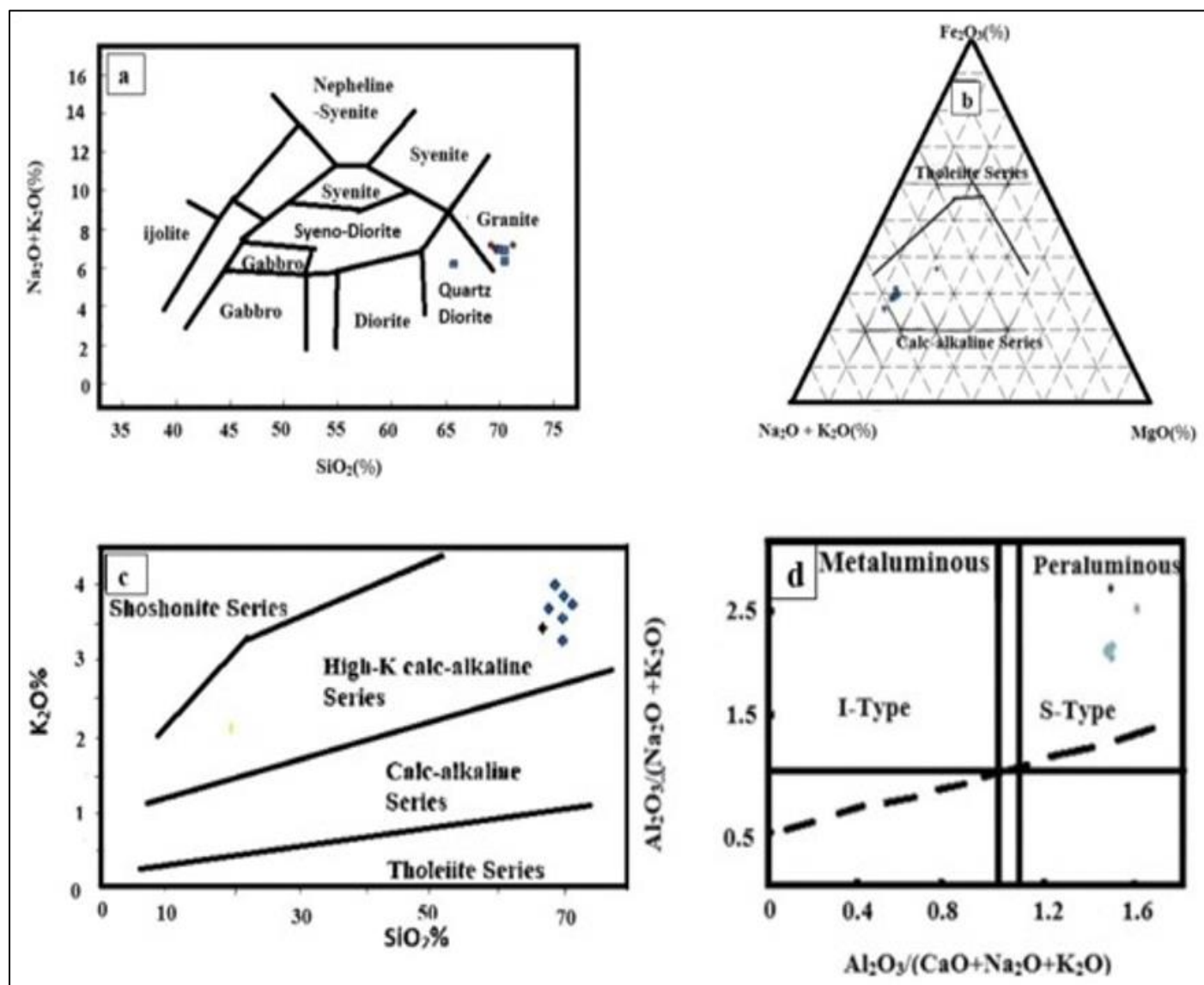


Fig 8 (a) Total Alkali versus SiO_2 diagram after (Cox et al.,1979),(b) AFM plot after (Irvine et al.,1971) showing the discrimination between calc-alkaline and tholeiitic series of the granitoids,(c) SiO_2 vs K_2O plot after Peccerillo and Taylor (1976); and (d) $Al_2O_3/(Na_2O+K_2O)$ versus $Al_2O_3/(CaO+Na_2O+K_2O)$ showing the granitoids plotted in the peraluminous field after (Frost et al.,2001).

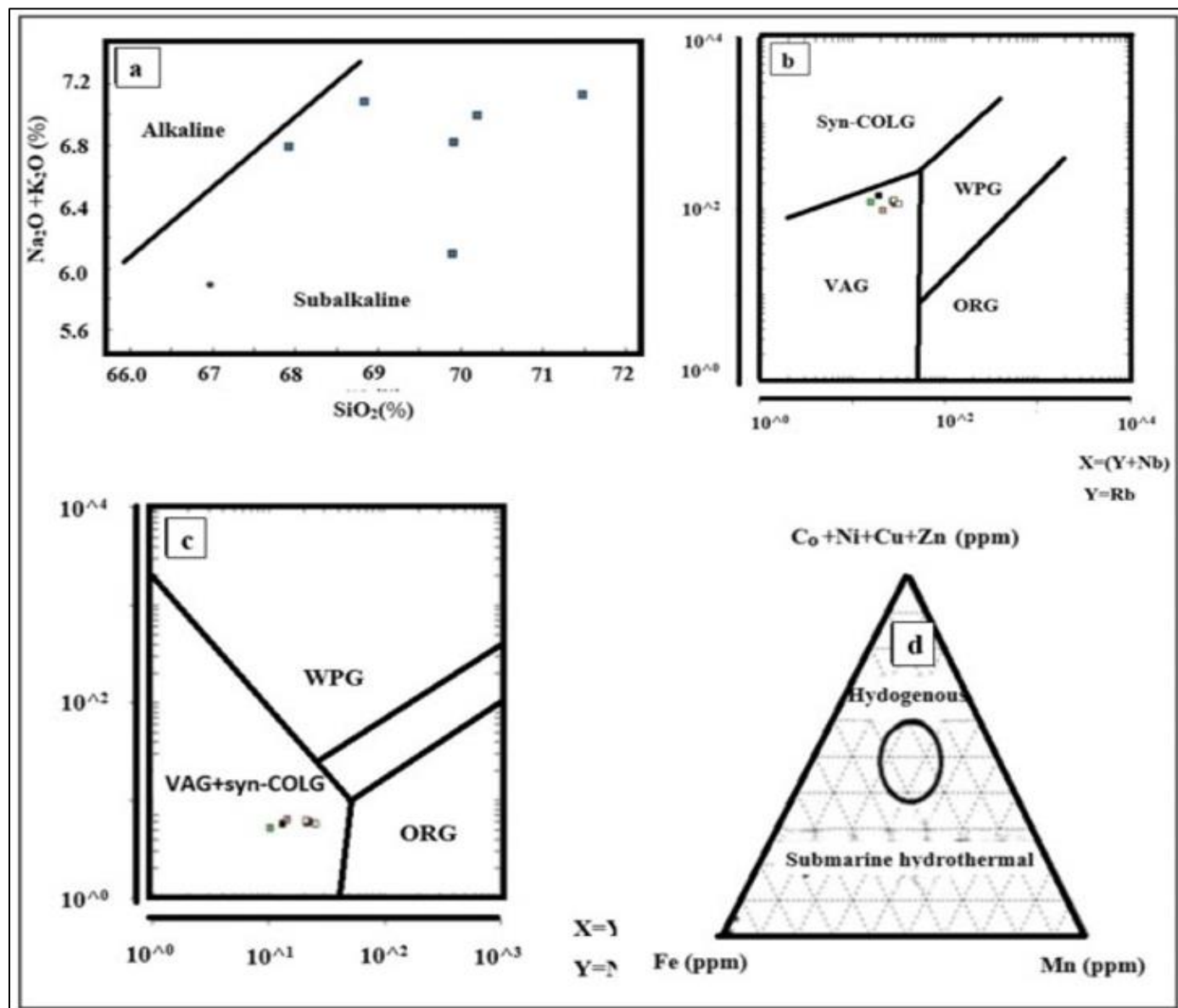


Fig 9 (a) $Na_2O + K_2O$ versus SiO_2 after McDonald and Katsura(1964), (b) $Y + Nb$ vs Rb tectonic discrimination diagram after (Pearce et al.,1984); (c)Discrimination diagram of (Pearce et al.,1984); (d) Ternary plot of $Co + Ni + Cu + Zn - Mn -Fe$ after (Bonatti et al., 1972).

Gold values in the granitoids are less than 0.001ppm and these values are low compared to average values of 0.004ppm in highly felsic granitoids (Turekian et al.,1961). The unmineralized granitoids are from the calc-alkaline series, peraluminous and form in a subduction zone.

➤ Quartz Veins

The trace elements in the quartz vein are presented in Tables 2.

Table 2 Elemental Composition (ppm) in Quartz Vein Around Gnimi-Yaboghan, Burkina Faso

Sample	YB005	YB002	GN008	GN010	GN009
Ag (ppm)	0.63	4.14	0.26	0.21	0.1
As(ppm)	7.7	99.6	65.5	3.7	1.2
Ba(ppm)	20	30	30	20	<10
Bi(ppm)	<0.01	3.34	1.2	0.03	0.02
Cd(ppm)	0.17	3.5	0.07	0.24	0.07
Ce(ppm)	0.61	0.54	1.27	0.27	0.36
Co(ppm)	0.5	0.2	1.1	0.6	0.3
Cr(ppm)	15	13	26	14	18
Cu(ppm)	5.6	9.2	5.5	7.8	1.9
Ga(ppm)	0.19	0.28	0.63	0.17	0.15

Hg(ppm)	<0.005	0.005	0.01	0.008	<0.005
Li(ppm)	0.5	0.7	1.2	0.7	0.2
Nb(ppm)	0.1	0.1	0.2	<0.1	<0.1
Ni(ppm)	1.8	1.2	3.8	4.6	1.6
Pb(ppm)	4.9	596	26.1	9.2	4.7
Rb(ppm)	1	0.8	3.2	0.4	0.2
Sb(ppm)	0.1	0.27	0.18	0.67	0.14
Sc(ppm)	0.1	0.1	0.5	0.1	<0.1
Se(ppm)	1	2	1	1	1
Sr(ppm)	3.9	4.4	4.4	1.3	2.2
Th(ppm)	0.11	0.08	0.27	0.05	0.04
V(ppm)	1	1	10	1	1
W(ppm)	<0.1	<0.1	1.7	0.1	0.1
Y(ppm)	0.3	0.1	0.8	0.2	0.1
Zn(ppm)	7	213	5	13	4
Zr(ppm)	0.8	0.5	3.9	<0.5	<0.5
Au(ppm)	0.009	9.9	0.019	0.515	<0.001

➤ *Origin and Gold Mineralization of the Quartz Vein*

Au values of <0.001ppm to 9.9ppm were recorded in the quartz veins and the Au was probably deposited during the granitic intrusion and the metamorphism of schist and amphibolite. The concentrations of (Co+Ni+Cu+Zn)- Fe-Mn in quartz veins were plotted on a ternary diagram proposed by (Bonatti et al.,1972) to differentiate between submarine hydrothermal and hydrogenous deposits. The plot indicates that the gold bearing quartz veins are of hydrothermal origin (Figure 9d.) .Most mineralized quartz veins are linked to hydrothermal process Clemens (2024).

The ratio of the lithophile elements Ba, Rb, K, and Sr has been used to investigate the nature of the fluid responsible for the gold mineralization (Danbatta et al.,2008). The K-Rb-

Ba signatures of the mineralising fluids were investigated in the studied samples (Table 3.). K/Ba values range from 5 to 23; K/Rb values range from 200 to 500, Ba/Rb values range from 20 to 50, and Rb/Sr values range from 0.1 to 0.73. These values are similar to results of (Ludtke et al.,1999) who reported average values of 285 for K/Rb; 36 for K/Ba; 7.8 for Ba/Rb; and 0.12 for Rb/Sr and according to these values the gold mineralization in the study area are controlled by structures an important tool for ore deposit exploration Vearncombe (2023) .The mineralized fluids from magmatic activities present a reduction of K/Rb and Rb/Sr values, Garrels and Mackenzie (1971)and maybe under physico-chemical conditions through fractures into cooler areas in the upper levels of the earth,the fractures were filled by the quartzAdebayo and Obasaju (2021).

Table 3 Selected elemental ratios in quartz vein around Gnimi-Yaboghan, Burkina -Faso

	YB005	YB002	GN008	GN010	GN009	Average
Sr	3.9	4.4	4.4	1.3	2.2	Average
K/Ba	10	7	23	5	11	11
K/Rb	200	250	219	250	500	284
Ba/Rb	20	37.5	9.4	50	45	32
Rb/Sr	0.26	0.18	0.73	0.31	0.1	0.3

V. DISCUSSION

Anomalous concentration of gold in the study area is hosted by the quartz veins, concentrations which were observed within the granitoids. The Au deposit is probably caused by hydrothermal fluids due to the deformation of pre-existing rocks such as the schist and the amphibolite. According to (Fontaine et al.,2017) gold deposits in South West, Burkina Faso, occur mainly in the volcano-sedimentary and schistose rocks, and the deformation of the schist and amphibolite facies was the consequence of the granitoids' intrusion (Debat et al.,2003 ; Naba et al.,2004). The emplacement of the granitoids played a key role during the gold deposit in the study area by being the source of the hydrothermal fluid which leached out the metals within quartz filled fractures under favorable physico-chemical conditions.

The K-Rb-Ba signatures of the mineralizing fluids suggest that the mineralization is controlled by structures during the granitoids emplacement. Gold mineralisation in the first deformation D1 was reported by (Perrouy et al.,2012).

VI. CONCLUSIONS

The present study revealed geologically four types of rocks: amphibolite, schist, granitoid and quartz vein.

From field observations, geochemical and fire assay analyses, it can be concluded that the gold mineralization is structurally controlled and hosted by quartz veins from hydrothermal submarine fluids and oriented NS to NE-SW. The emplacement of granitoids within the Boromo belt, where the study area is located, (Ouedraogo et al.,2022) is the source of mineralized hydrothermal fluids (Holden et

al.,2011) that contributed to the formation of quartz vein mineralization within fractures. This suggests that gold mineralization is likely associated with the granitoid intrusion, which affected the surrounding schist and amphibolite, allowing mineralized fluids to migrate through the fractures. While the granitic rocks themselves are unmineralized, the quartz veins exhibit significantly higher gold concentrations, reaching up to 9.9 ppm.

ACKNOWLEDGEMENTS

I would like to thank the African Union Commission (AUC) for financing this work from the beginning to the end. I am also grateful to the Pan African University of Life and Earth Science Institute (Including Health and Agriculture), University of Ibadan, Ibadan, Oyo State, Nigeria and the Department of Geology, University of Ibadan, for the welcome and comfort.

➤ Conflict of Interests

I declare that there is not a conflict of interest in this research project.

➤ Funding

This work was supported by the African Union Commission

REFERENCES

- [1]. Goldfarb, R.J., Groves, D.I., Gardoll, S. Orogenic gold and geologic time: A global synthesis: *Ore Geology Reviews* 2001; 18, Pp. 1–75.
- [2]. Béziat, D., Dubois, M., Debat, P., Nikiéma, S., Salvi, S., and Tollon, F. Gold metallogeny in the Birimian craton of Burkina Faso (West Africa). *Journal of African Earth Sciences*, 2008; 50(2–4), 215–233. <https://doi.org/10.1016/j.jafrearsci.2007.09.017>.
- [3]. Baratoux, L., Metelka, V., Naba, S., Ouyi, P., Siebenaller, L., Jessell, M.W., Nare, A., Salvi, S., Beziat, D., Franceschi, G. Tectonic evolution of the Gaoua region, Burkina Faso: Implications for mineralization. *Journal of African Earth Sciences* 2015; Volume 112, pp. 419–439.
- [4]. Markwitz, V., Hein, K. A. A., Jessell, M. W., and Miller, J. Metallogenic portfolio of the West Africa craton. *Ore Geology Reviews*, 2016, 78, 558–563. <https://doi.org/10.1016/j.oregeorev.2015.10.024>
- [5]. Ilboudo, H., Sawadogo, S., Traoré, A. S., Sama, M., Wenmenga, U., & Lompo, M. Intrusion-related gold mineralization: Inata gold deposit, Bélahourou district, Northern Burkina Faso (West-Africa). *Journal of African Earth Sciences* 2018; 148, 52–58. <https://doi.org/10.1016/j.jafrearsci.2018.05.015>
- [6]. Oke, S. A., Abimbola, A. F., & Rammlair, D. Mineralogical and Geochemical Characterization of Gold Bearing Quartz Veins and Soils in Parts of Maru Schist Belt Area, Northwestern Nigeria. *Journal of Geological Research* 2014; Arti(<http://dx.doi.org/10.1155/2014/314214>).
- [7]. Gustafson, L. B. (1989). SEG distinguished lecture in applied geology the importance of structural analysis in gold exploration. *Economic Geology*, 84(4), 987–993. <https://doi.org/10.2113/gsecongeo.84.4.987>
- [8]. Nguimatsia, F. W. D., Bolarinwa, A. T., Yongue, R. F., Ndikumana, J. de D., Olajide-Kayode, J. O., Olisa, O. G., Abdu-Salam, M. O., Kanga, M. A., Djou, E. S. Diversity of Gold Deposits, Geodynamics and Conditions of Formation: A Perspective View. *Open Journal of Geology* 2017; 07(11), 1690–1709. <https://doi.org/10.4236/ojg.2017.711113>
- [9]. Lovering, S. Epigenetic, diplogenic, singenic, and lithogene deposits. *Economic Geology* (1963); V.58, PP.315–331
- [10]. Ouyi, P., Siebenaller, L., Salvi, S., Beziat, D., Naba, S., Baratoux, L., Nare, A., Franceschi, G., 2016. The Nassara gold prospect, Gaoua District, southwestern Burkina Faso. *Ore Geol. Rev.* 78, 623e630.
- [11]. Koffi, Y. H., Djro, S. C., Wenmenga, U. Lithostructural and Petrochemical Survey of Djarkadougou Gold Prospect (South West Burkina Faso /West Africa). *Earth Science Research* 2017; 6(1), 155. <https://doi.org/10.5539/esr.v6n1p155>
- [12]. Ali, R., Isdine, D., Hermann, I., Séta, N. Nouvelles données lithologiques et structurales du secteur de Nindangou dans le prolongement Est de la ceinture de Goren (Burkina Faso-Afrique de l' Ouest). *Bulletin de l'Institut Scientifique* · November 2022
- [13]. Castaing, C., Billa, M., Milesi, J., Thieblemont, D., Le Mentour, J., Egal, E., Donzeau, M., Guerrot, C., Cocherie, A., Chevremont, P. Notice explicative de la carte géologique et minière du Burkina Faso à 1/1,000,000. BRGM BUMIGEB, 2003; 147.
- [14]. Ouedrago, G. E., Joseph, U., Zerbo, K., Geosciences, L., Zongo, H. G., Joseph, U., Zerbo, K., and Geosciences, L. Structural Evolution and Its Implication for the Emplacement of Gold Deposit in the Central Part of Burkina Faso, West Africa. *ESI Preprints* 2023; 458.
- [15]. Ledru, P., Feybesse, J., Dommanget, A., Marcoux, E., Codex, O. (1992). Early Proterozoic ore deposits and tectonics of the Birimian orogenic belt, West Africa. *58, Precambrian Research*, 58 (1992) 305–344 305 Elsevier Science Publishers B.V., Amsterdam
- [16]. Block, S., Ganne, J., Baratoux, L., Zeh, A., Jessell, M., Ailleres, L., Siebenaller, L., Toulouse, G. E., Diop, C. A., and Road, W. (2015). Petrological and geochronological constraints on lower crust exhumation during Paleoproterozoic (Eburnean) orogeny, NW Ghana, West African Craton. *J. Metamorphic Geol.*, 33, 463–494. <https://doi.org/10.1111/jmg.12129>
- [17]. Nancy, I. (1990). A Major 2.1 Ga Event of Mafic Magmatism in West Africa: An Early Stage of Crustal Accretion regions from the mantle that growth from of sinking mobile of the Ahaggar [Lancelot work by Boher data, 1990) have shown major series of orogenic episodes: (1) the Liberian The polycyclic crustal growth in West Africa. 95.
- [18]. Boher, M., Abouchami, W., Michard, A., Albarede, F., Arndt, N.T., 1992. Crustal growth in West Africa at 2.1 Ga. *J. Geophys. Res. B Solid Earth Planets* 97, 345e369.

- [19]. Ganne, J., Gerbault, M., Block, S., 2014. Thermo-mechanical modeling of lower crust exhumation-Constraints from the metamorphic record of the Palaeoproterozoic Eburnean orogeny, West African Craton, *Precambrian Research*, 243, 88–109.
- [20]. Caby, R., Delor, C., & Agoh, O. (2000). Lithologie, structure et métamorphisme des formations birimiennes dans la région d'Odiène (Côte d'Ivoire): Role majeur du diapirisme des plutons et des décrochements en bordure du craton de Man. *Journal of African Earth Sciences*, 30(2), 351–374. [https://doi.org/10.1016/S0899-5362\(00\)00024-5](https://doi.org/10.1016/S0899-5362(00)00024-5)
- [21]. Tounkara et al. (2017). Structural and Lithological Study of Gold Mineralization in the Areas of Bena and. *Open Journal of Geology*, 7, 1318–1326. <https://doi.org/10.4236/ojg.2017.79087>
- [22]. Abouchami et al., (1990). A Major 2.1 Ga Event of Mafic Magmatism in West Africa: An Early Stage of Crustal Accretion regions from the mafic that growth from of sinking mobile of the Ahaggar [Lancelot work by Boher data, 1990] have shown major series of orogenic episodes. *Journal OF Geophysical Research*, VOL. 95, NO. B I 1, PAGES 17,605-17,629, OCTOBER 10, 1990
- [23]. Oberth, T. Ulrich Vetter, Donald W. Davis, Joe A. Amanor, (1998). Age constraints on gold mineralization and Paleoproterozoic crustal evolution in the Ashanti belt of southern Ghana. *Precambrian Research* 89 (1998) 129- 143
- [24]. Dabo M. et Aïfa, T. (2011). Late Eburnean deformation in the KoliaBoboti sedimentary basin, Kédougou-Kéniéba Inlier, Sénégal. *Journal of African Earth Sciences*, 60, 106-116, doi:10.1016/j.jafrearsci.2011.02.005.
- [25]. Chris Raplph, (2013). Birimian Greenstone Belt of West Africa-june 2013 (Vol.82.No.10)-ICMJ^{rs} Prospecting and Mining Journal.
- [26]. Augustin, J., Gaboury, D., & Crevier, M. (2015). The world-class Wona-Kona gold deposit, Burkina Faso. *Ore Geology Reviews*, <https://doi.org/10.1016/j.oregeorev.2015.10.017>
- [27]. Block, S., Jessell, M., Aillères, L., Baratoux, L., Bruguier, O., Zeh, A., Bosch, D., Caby, R., Mensah, E., 2016. Lower crust exhumation during Paleoproterozoic (Eburnean) orogeny, NW Ghana, West African Craton: interplay of coeval contractional deformation and extensional gravitational collapse. *Precambrian Research*. Volume 274, pp. 82–109.
- [28]. Jessell, M. W. (2018). 100 years of research on the West African Craton *Journal of African Earth Sciences* 100 years of research on the West African Craton. October 2015. <https://doi.org/10.1016/j.jafrearsci.2015.10.008>
- [29]. Seta Naba, Martin Lompo, Pierre Debat, Jean Luc Bouchez, Didier Beziat (2004). Structure and emplacement model for late-orogenic Paleoproterozoic Structure and emplacement model for late-orogenic Paleoproterozoic granitoids: the Tenkodogo – Yamba elongate pluton (Eastern Burkina Faso). *Journal of African Earth Sciences* 38 (2004)41–57 <https://doi.org/10.1016/j.jafrearsci.2003.09.004>.
- [30]. Reisberg, L., Le Mignot, E., Andre-Mayer, A.S., Miller, J., Bourassa, Y., 2015. Re-Os geochronological evidence for multiple Paleoproterozoic Gold mineralizing events at the scale of the West African Craton. In: *Proceedings of the 13th SGA Biennial Meeting, Nancy, 24-27 August 2015*, 4, pp. 1655e1658.
- [31]. Hein, K. A. A., Morel, V., Kagon, O., Kiemde, F., & Mayes, K. (2004). Birimian lithological succession and structural evolution in the Goren segment of the Boromo – Goren Greenstone Belt, Burkina Faso. 39, 1–23. <https://doi.org/10.1016/j.jafrearsci.2004.05.003>
- [32]. Metelka, V., Baratoux, L., Naba, S., Jessell, M. W. (2011). A geophysically constrained litho-structural analysis of the Eburnean greenstone belts and associated granitoid domains, Burkina Faso, West Africa. *Precambrian Research*, 190(1–4), 48–69. <https://doi.org/10.1016/j.precamres.2011.08.002>
- [33]. Chudasama, B., Porwal, A., Kreuzer, O. P., and Butera, K. (2015). Geology, geodynamics and orogenic gold prospectivity modelling of the Paleoproterozoic Kumasi Basin, Ghana, West Africa. *Ore Geology Reviews*, 20. <https://doi.org/10.1016/j.oregeorev.2015.08.012>
- [34]. Lüdtke, G., Hirdes, W., Konan, G., Kone, Y., N'da, D., Traore, Y., Zamble, Z., 1999. Geologie de la région Haute Comoe Suddfeuilles Dabakala (2b, d et 4b,d). *Di rection de la Geologie Abidjan Bulletin*, p. 176.
- [35]. Béziat, D., Bourges, F., Debat, P., Lompo, M., Martin, F., and Tollon, F. A Paleoproterozoic ultramafic-mafic assemblage and associated volcanic rocks of the Boromo greenstone belt: Fractionates originating from island-arc volcanic activity in the West African craton. *Precambrian Research*, 2000; 101(1), 25–47. [https://doi.org/10.1016/S0301-9268\(99\)00085-6](https://doi.org/10.1016/S0301-9268(99)00085-6)
- [36]. Ilboudo, H., Sawadogo, S., Kagambega, N., and Remmal, T. Petrology, geochemistry, and source of the emplacement model of the Paleoproterozoic Tiébéle Granite Pluton, Burkina Faso (West-Africa): contribution to mineral exploration. *International Journal of Earth Sciences*, 2021;110(5),1753–1781. <https://doi.org/10.1007/s00531-021-02039-3>
- [37]. Masurel, Q., Eglinger, A., Thébaud, N., Allibone, A., Mcfarlane, H., Miller, J., Jessell, M., Aillères, L., Vanderhaeghe, O., Masurel, Q., Eglinger, A., Thébaud, N., and Allibone, A. Paleoproterozoic gold events in the southern West African Craton: review and synopsis (2021).
- [38]. Baratoux, L., Mételka, V., Naba, S., Jessell, M.W., Grégoire, M. and Ganne, J. (2011) Juvenile Paleoproterozoic Crust Evolution during the Eburnean Orogeny (~2.2-2.0 Ga), Western Burkina Faso. *Precambrian Research*, 191, 18-45. <https://doi.org/10.1016/j.precamres.2011.08.010>
- [39]. Cox, K.G., Bell, J.D., Pankhurst, R.J., 1979. The interpretation of igneous rocks. *Allen & Unwin*, p. 1-464.
- [40]. Irvine, T.N., Baragar, W.R.A. A guide to the chemical classification of the common volcanic rocks.

- Canadian Journal of Earth Sciences 1971; 8, Pp. 523-548.
- [41]. Peccerillo, A., Taylor, S.R. Geochemistry of Eocene calc-alkaline volcanic rocks from the Kastamonu area, Northern Turkey. *Contributions to Mineralogy and Petrology*, 1976; 58, Pp. 63-81.
- [42]. Frost, B.R., Barnes, C.G., Collins, W.J., Arculus, R.J., Ellis, D.J., Frost, C.D. A geochemical classification for granitic rocks. *Journal of Petrology* 2001;42, Pp. 2035-2048.
- [43]. Frost, B.R., Frost, C.D.. A Geochemical Classification for Feldspathic Igneous Rocks. *Journal of Petrology*, 2008;11, Pp. 1955-1969.
- [44]. Debon, F., Le Fort, P. A chemical–mineralogical classification of common plutonic rocks and associations. *Transactions of the Royal Society of Edinburgh, Earth Sciences*, 1983; 73, Pp. 135–149.
- [45]. McDonald, G.A., Katsura, T. Chemical composition of Hawaiian lavas. *Journal of Petrology* 1964;5, 82-113.
- [46]. Pearce, J.A., Harris, N.B.W., Tindle, A.G. Trace element discrimination diagrams for the tectonic interpretation of granitic rocks. *Journal of Petrology* 1984; 25, Pp. 217-235.
- [47]. Pearce, J.A. A user's guide to basalt discrimination diagrams. In: WYMAN, D. A. (ed.): *Trace Element Geochemistry of Volcanic Rocks: Applications for Massive Sulphide*, 1996.
- [48]. Bonatti, T. Kraemer, and H. Rydell, "Classification and genesis of submarine iron-manganese deposits," in *Proceedings of the Conference on Ferromanganese Deposits on the Ocean Floor*, D.R. Horn, Ed., 1972; pp. 149–166, Arden House, Harriman, NY, USA.
- [49]. Turekian, K.K., Wedepohl, K.H. Distribution of the Elements in Some Major Units of the Earth's Crust. *Geological Society of America Bulletin*, 1961;72, Pp. 175-192.
- [50]. J. D. Clemens (13 Nov 2024): Igneous reasons why porphyry Cu–Au deposits are not magmatic, *Australian Journal of Earth Sciences*, DOI: 10.1080/08120099.2024.2422433
- [51]. Danbatta, U. A., Abubakar, Y. I., and Ibrahim, A. A.. Geochemistry of Gold Deposits in Anka Schist Belt, Northwestern, Nigeria. *Nigerian Journal of Chemical Research* 2008 ;13.
- [52]. J. R. Vearncombe (2023) Function and status of structural geology in the Resource industry, *Australian Journal of Earth Sciences*, 70:7, 908-931, DOI: 10.1080/08120099.2023.22149
- [53]. Garrels, R. M. and MacKenzie, F.T., *Evolution of Sedimentary Rocks* 1971; p. 394, Norton and Co., New York.
- [54]. Adebayo, S., and Obasaju, D. Geological and Geochemical Prospecting for Gold Mineralization in Bode-Saadu Axis, Southwestern Nigeria. *GeoScience Engineering* 2021; 67(3), 64–76. <https://doi.org/10.35180/gse-2021-0053>
- [55]. Fontaine, A., Eglinger, A., Ada, K., Andre-Mayer, A-S., Reisberg, L., Siebenaller, L., Le Migot, E., Ganne, J., Poujol, M. Geology of the world-class Kiaka polyphase gold deposit, West African Craton, Burkina Faso. *Journal of African Earth Sciences* 2017; Volume 126, pp. 96-122.
- [56]. Debat, P., Nikiema, S., Mercier, A., Lompo, M., Beziat, D., Bourges, F., Roddaz, M., Salvi, S., Tollon, F., Wenmenga, U. A new metamorphic constraint for the Eburnean orogeny from Paleoproterozoic formations of the Man shield (Aribinda and Tampilga countries, Burkina Faso). *Precambrian Research* 2003; Volume 123, p. 47–65
- [57]. Perrouty, S., Ailleres, L., Jessell, M.W., Baratoux, L., Bourassa, Y., Crawford, B. Revised Eburnean geodynamic evolution of the gold-rich southern Ashanti Belt, Ghana, with new field and geophysical evidence of pre-Tarkwaian deformations. *Precambrian Research* 2012 : Volume 204-205, pp. 12-39.
- [58]. Ouedraogo, T., Sawadogo, S., and Kiéma, B. La minéralisation aurifère de Napélépéra, SW Burkina Faso, Afrique de l' Ouest : mise en place dans une zone de cisaillement tardi-orogénique Éburnéenne. *Résumé. Afrique SCIENCE* 2022; 20(1), 81–92.
- [59]. Holden, E., Wong, J. C., Kovesi, P., Wedge, D., Dentith, M., and Bagas, L. Identifying structural complexity in aeromagnetic data : An image analysis approach to green fields gold exploration. *Ore Geology Reviews* 2012 ;46, 47–59. <https://doi.org/10.1016/j.oregeorev.2011.11.002>